Food and Chemical Toxicology 181 (2023) 114088

Contents lists available at ScienceDirect

Food and Chemical Toxicology

journal homepage: www.elsevier.com/locate/foodchemtox

Rapid identification of counterfeited beef using deep learning-aided spectroscopy: Detecting colourant and curing agent adulteration

Eunjung Jo[a,b,1], Youngjoo Lee[a,1], Yumi Lee[a], Jaewoo Baek[a], Jae Gwan Kim[a,*]

[a] Department of Biomedical Science and Engineering, Gwangju Institute of Science and Technology (GIST), 123 Cheomdangwagi-ro, Buk-gu, Gwangju, 61005, Republic of Korea

[b] Department of Artificial Intelligence, Korea University, 145 Anam-ro, Seongbuk-gu, Seoul, 02841, Republic of Korea

ARTICLE INFO

Handling Editor: Dr. Bryan Delaney

Keywords:
Diffuse reflectance spectra
Deep learning
Meat safety
Food fraud
Colourant
Curing agent

ABSTRACT

The adulteration of meat products using colourants and curing agents has heightened concerns over food safety, thereby necessitating the development of advanced detection methods. This study introduces a deep-learning-based spectroscopic method for swiftly identifying counterfeit beef altered to appear fresh. The experiment involved 60 beef samples, half of which were artificially adulterated using a colouring solution. Despite meticulous analysis of the beef's colour attributes, no significant differences were observed between the fresh and adulterated samples. However, our method, utilising a 344–1040 nm spectral range, achieved a classification accuracy of 98.84%. To enhance practicality, we employed gradient-weighted class activation mapping and identified the 580–600 nm range as particularly influential for classification. Remarkably, even when we narrowed the input to the model to this spectral range, a high level of classification accuracy was maintained. To further validate the model's robustness and generalisability, we allocated 70 beef samples to an external validation set. Comparative performance analysis revealed that our model outperformed traditional machine learning algorithms, such as SVM and logistic regression, by 9.3% and 28.4%, respectively. Overall, this study offers invaluable insights for detecting counterfeited beef, thereby contributing to the preservation of meat product quality and integrity within the food industry.

1. Introduction

Food fraud presents a substantial challenge posing threats to both public health and the international economy (Spink and Moyer, 2013; Hellberg et al., 2020; Li et al., 2023). This fraudulent activity, characterised by the intentional deception of consumers for financial advantages, is estimated to cost between $10 billion and $15 billion annually, accounting for approximately 10% of all marketed food products (Johnson, 2014; Robson et al., 2020). Meat products, in particular, frequently fall victim to this form of fraud, owing to their elevated consumer demands and high selling prices (Barai et al., 1992; Robson et al., 2020).

One prevalent type of meat fraud (Type 1) entails the contamination of meat by amalgamating cheaper cuts with more expensive ones, as a strategy to decrease costs (Cavin et al., 2018; Fengou et al., 2021). Another category of meat fraud (Type 2) involves utilising inexpensive, readily available colourants or curing agents to disguise inferior quality meat as a higher-value product (Spink et al., 2017; Li et al., 2022). This latter form of meat fraud (Type 2) is particularly pernicious for consumers as the colour of the meat significantly influences their purchasing decisions (Font-i Furnols and Guerrero, 2014; Bjelanovic et al., 2016; Corlett et al., 2021). Furthermore, several colourants or curing agents employed in such fraudulent practices are known to endanger consumer health (Jia and Jukes, 2013; Clofent et al., 2020; Shakil et al., 2022). For instance, certain colourants, such as Sudanese dyes, have been prohibited in numerous countries owing to their toxic implications (Pan et al., 2012; Barciela et al., 2023). Reports also suggest that curing agents, such as sodium nitrite and sodium ascorbate, may be linked to colorectal cancer (Desmond, 2006; Santarelli et al., 2008; Crowe et al., 2019). However, the majority of studies addressing meat fraud focus on meat adulteration (Type 1) and neglect the distinction between artificially coloured beef and fresh beef (Type 2) (Kamruzzaman et al., 2016; Hong et al., 2017; Zheng et al., 2019). Considering the critical role of meat colour in consumer purchasing decisions and the potential health

* Corresponding author.
E-mail address: jaekim@gist.ac.kr (J.G. Kim).

[1] Eunjung Jo and Youngjoo Lee contributed equally to this work.

https://doi.org/10.1016/j.fct.2023.114088
Received 26 July 2023; Received in revised form 20 September 2023; Accepted 4 October 2023
Available online 5 October 2023

hazards associated with artificial colouring ingredients, there is an urgent need to explore and develop reliable methods for detecting counterfeit meat.

Spectroscopic methodologies are widely acclaimed for addressing food safety concerns, owing to their capacity to provide comprehensive insights into the compositions and traits of various substances (Mitsumoto et al., 1991; Giana et al., 2003; Mandair and Morris, 2015; Qu et al., 2015; Petronijević et al., 2017; Petersen et al., 2021). For instance, the efficiency of near-infrared spectroscopy, fluorescence spectroscopy, and hyperspectral imaging in the analysis and evaluation of the quality of diverse food products such as mushrooms, tea, fruit, and milk has already been established (Wang and Paliwal, 2007; Aernouts et al., 2011; Huang et al., 2014; Meenu and Xu, 2019; Firmani et al., 2019; Walsh et al., 2020; Matveyeva et al., 2022). Nevertheless, several limitations persist that hinder the deployment of these technologies within the food industry. Hyperspectral imaging, for instance, faces substantial barriers to its widespread adoption, including elevated acquisition costs, intricate data analysis prerequisites, and protracted image acquisition and processing durations (Gowen et al., 2007; Roberts et al., 2018). Similarly, near-infrared and fluorescence spectroscopy are susceptible to environmental variables such as temperature, humidity, and mechanical vibration, thereby complicating their industrial application (Agelet et al., 2010; Hassoun et al., 2019).

In recent years, diffuse reflectance spectroscopy (DRS) has emerged as a viable technique for analysing meat quality, serving to mitigate the limitations inherent in the aforementioned spectroscopic information-based methodologies (Nguyen et al., 2016, 2019; Nguyen and Kim, 2019; Shin et al., 2021). This approach places a particular emphasis on myoglobin, a heme protein responsible for oxygen transport in muscle cells. As myoglobin experiences changes in its redox forms over time, it becomes an indispensable factor in the analysis of beef quality (Jurgens et al., 2000; Shin et al., 2021).

However, the application of DRS during beef quality analysis, despite its encouraging results, is currently limited by the intricacies involved in extracting myoglobin information (Nguyen et al., 2019; Shin et al., 2021). The process involves fitting an analytical photon diffusion model to the recorded diffuse reflectance spectra using a non-linear least-squares method, the complexity of which hinders the practical implementation of DRS-based methodologies in industrial or real-world environments. Although, spectroscopic techniques have been acknowledged as valuable tools across various industries, including the food sector, their application for detecting counterfeit meat remains under-explored. Consequently, reliable, straightforward spectroscopic methodologies that can directly utilise spectral information for identifying counterfeit meat, circumventing the need for complex myoglobin information extraction, are urgently required.

Deep-learning (DL) models, particularly convolutional neural networks (CNNs), have emerged as potent tools for classification tasks, surpassing conventional analysis methods in numerous domains (Krizhevsky et al., 2012; He et al., 2016; Islam et al., 2020; Gautam and Raman, 2021). CNNs have demonstrated extraordinary performance not only in medical and signal analysis (Drugman et al., 2015; Xu et al., 2020) but also in the food industry. Several studies, including our own previous study (Shin et al., 2021), have utilised CNNs for food safety evaluation and quality control (Moon et al., 2020; Liu et al., 2021; Chakravartula et al., 2022). In our previous study (Shin et al., 2021), we successfully demonstrated the potential of AlexNet, a CNN-based architecture, in extracting freshness-related features from the spectral information of beef. Furthermore, it was able to accurately classify the freshness of beef with remarkable accuracy (ACC = 91.9%). These results provide significant insights into the potential application of DL in the analysis of beef spectral data, paving the way for precise detection of counterfeit beef.

Given the demonstrated efficiency of DRS in meat quality analysis and the robust feature extraction capabilities of DL from spectral information, we propose an AlexNet-based DL model for the detection of counterfeit beef using diffuse reflectance spectra directly. To assess the performance of our proposed method, we prepared a colouring solution using a mixture of colourants and curing agents. We then established two groups: a counterfeit group treated with the colouring solution and a standard group without such treatment. The model was trained on spectral data gathered from both groups. Notably, the model was able to discern an optimal pattern for counterfeit beef classification using only the diffuse reflectance spectra, without the need for supplemental myoglobin information. This approach confirms the feasibility and practicality of our proposed method in industrial or real-world applications. Furthermore, we employed gradient-weighted class activation mapping (Grad-CAM), a technique used to visualise significant regions of input data that strongly influence the model's decision making (Selvaraju et al., 2017). This method was utilised to determine the wavelength regions playing an integral role in the classification of counterfeit beef.

To the best of our knowledge, this study represents a pioneering effort to directly exploit spectral information for the detection of counterfeit beef. By accurately capturing important features from the diffuse reflectance spectra, we achieved a high degree of accuracy in distinguishing fresh beef from counterfeit beef. The integration of DRS and DL in this study presents a reliable and pragmatic solution for detecting counterfeit beef. This method not only serves to prevent the consumption of counterfeit products but also safeguards consumer health and fortifies trust in the food industry.

2. Materials and methods

2.1. Sample preparation and storage conditions

For our experimental process, we purchased 60 beef samples extracted from the rump sections of three cows, all slaughtered on the same day, from a local butcher shop in Gwangju, South Korea. The beef samples were stored in an ice-filled cooler and transported to the laboratory within 30 min. Each sample was subsequently cut into 2 cm × 2 cm × 2 cm (length × width × thickness) portions and packaged in a polyethylene sheet with low oxygen permeability. The samples were then stored in a refrigerator at 4 °C for a duration of 13 days. These 60 beef samples are referred to as the internal set in this study.

2.2. Preparation of the colouring solution and beef dyeing procedures

The preparation of the colouring solution followed an empirical process, drawing on insights obtained from prior reports and conducting repeated experiments to attain a colour closely resembling that of fresh beef (Epley et al., 1992). The colouring solution consisted of sodium nitrite ($NaNO_2$, 60 mg, Sigma-Aldrich, USA), sodium ascorbate ($C_6H_7NaO_6$, 149.5 mg, Sigma-Aldrich, USA), Red No. 40 food colourant ($C_{18}H_{14}O_8N_2S_2Na_2$, 4 mg, Littes, South Korea), and natural squid ink colourant (6 mg, Next Innovation Food, Republic of Korea) combined with 80 ml of purified water. Among the 60 beef samples, half were designated as the counterfeit group and were submerged in the colouring solution for a duration of 1 h on day 11. The remaining samples, identified as the standard group, were not treated by the colouring solution. Following the colouring process, the samples in the counterfeit group were allowed a 2-day reaction period to ensure comprehensive staining of the beef's surface by the colouring solution.

2.3. Analysis of the colour information

Colour images of the beef samples were captured using a Samsung SEC-NX3000 camera (Republic of Korea) for red, green, and blue (RGB) analysis. To control environmental variables, all images were captured within a mini-studio (RM-PB6060, RAMI, Republic of Korea). The camera settings were configured to a focal length of 30 mm, exposure time of 1/50, and a f-number of f/5.6, with a resolution of 5427 × 3648 pixels. The centre of each image was cropped to 100 × 100 pixels, and the intensity of the RGB components from each pixel was extracted to estimate the average intensity of the cropped region. The derived average intensity values served to confirm that, upon visual examination, the counterfeit group was indistinguishable from the standard group. The methodologies described in this section were implemented using Python software.

2.4. Diffuse reflectance spectra acquisition system

The DRS system deployed for this study comprised a spectrometer (USB4000, Ocean Optics, Delray Beach, FL, USA), which collected light within a wavelength range of 344–1040 nm, and a broadband light source (Tungsten halogen lamp, HL-2000-HP, Ocean Optics, Delray Beach, FL, USA). An optical probe equipped with two optical fibres (each with a diameter of 200 μm) at a separation distance of 2 mm was connected to the light source and the spectrometer. This probe was placed on the beef samples to obtain the diffuse reflectance spectra. To prevent the contamination of the beef samples by the optical probe, the samples were placed on a 1-mm-thick acrylic plate during the measurement process. The beef sample spectra (R_{sample}) were recorded at 5 p.m., at 24-h intervals from the day of the beef samples' arrival (day 0). The probe was shielded with a black fabric to eliminate any influence of ambient light on the measurements.

2.5. Statistical analysis

To affirm the effectiveness of the colouring solution, we performed a statistical comparison of the colour information between fresh (day 1) and counterfeit (day 13) beef samples within the counterfeit group. The analysis focused on the intensity of the RGB components extracted from the beef surface images. A paired *t*-test with Bonferroni correction was employed to examine the changes in colour information within the counterfeit group, comparing the intensities of the RGB values before and after the application of the colouring solution (Mishra et al., 2019). The same statistical methodology was applied to the standard group to monitor the change in colour information in the absence of the colouring solution. Moreover, an independent *t*-test on the colour information was carried out to confirm the consistency in sample preparation and storage conditions between the standard and counterfeit groups.

To ensure the appropriate selection of standard and counterfeit data for model training and testing, we applied a paired *t*-test with Bonferroni correction. This process involved determining whether the data from different days must be included in the training and testing phases based on the colour information of the standard beef samples from day 1, a procedure elaborated upon in Section 2.6.

2.6. Model architecture and classification mechanism

The AlexNet architecture, known for its effectiveness in various classification tasks, employs Convolutional Neural Networks (CNNs) (Jogin et al., 2018). Utilised for its feature extraction capabilities, AlexNet was applied in our study to classify beef samples as either counterfeit or standard based on their diffuse reflectance spectra (R_{sample}). The architecture extracted key features from R_{sample}, which were then transformed into class probabilities through fully connected (FC) layers. We applied activation functions, such as sigmoid, to the FC layers, thereby converting the extracted features into a format interpretable as the class probabilities. These probabilities, generated by the sigmoid function, subsequently facilitated the categorisation of each sample into the most probable class (either standard or counterfeit). The kernel size and stride parameters of the AlexNet model were optimised to ensure efficient and accurate processing of the diffuse reflectance spectra.

$$P(x) = Sigmoid\left(FC\left(model\left(R_{sample}\right)\right)\right) \tag{1}$$

where the diffuse reflectance spectra, R_{sample}, are represented by dimensions of $R_{sample} \in R(1 \times 3647)$. The model executes the feature extraction process, denoted by $model(\bullet)$. Subsequently, the extracted features are analysed by the FC layer (denoted as $FC(\bullet)$) to ascertain the class probability. Ultimately, the likelihood of the input belonging to a specific class is determined via the sigmoid function ($Sigmoid(\bullet)$), represented as $P(\bullet)$.

The model proposed in this study, based on the AlexNet architecture, was trained using a stratified 5-fold cross-validation manner to ensure an even representation of both standard and counterfeit beef samples in both the training and testing subsets. Our dataset consisted of a total of 210 samples, comprising 180 standard beef samples and 30 being counterfeit beef samples. To address the class imbalance issue, we implemented class-specific weight normalisation during the training process. The class-specific weights are determined based on the number of samples in each class and can be calculated using the following formula:

$$W'_{c_i} = \frac{1 - number\ of\ sampels\ in\ C_i}{total\ number\ of\ samples} \tag{2}$$

where W'_{c_i} represents the normalised weight for the *i*-th class (C_i), which signifies whether it represents counterfeit or standard.

To designate the standard class, we carried out a statistical test that compared the colour information of the beef samples on day 1 with that from the subsequent days. According to the results of this statistical test, as illustrated in Table 1, the colour information of the beef samples on day 2 and day 3 did not significantly deviate from that on day 1. Consequently, these samples were categorised as standard and were incorporated into the dataset for model training and testing.

For the optimisation of the model's performance, a learning rate of 0.0001 was employed in tandem with the Adam optimiser for weight updates. A batch size of 64 and an epoch size of 100 were designated for training. Activation functions were applied to each layer, and all DL models were implemented using Python 3.7.

2.7. Comparison metrics

To ascertain the performance of the model, four key metrics were utilised: sensitivity, specificity, F1-score, and area under the curve (AUC).

$$Sensitivity = \sum_{i=1}^{n} \frac{1}{n} \frac{TP_i}{TP_i + FN_i} \tag{3}$$

$$Specificity = \sum_{i=1}^{n} \frac{1}{n} \frac{TN_i}{TN_i + FP_i} \tag{4}$$

$$F1 - score = \sum_{i=1}^{n} \frac{1}{n} \frac{2TP_i}{2TP_i + FP_i + FN_i} \tag{5}$$

where TP represents true positives, TN stands for true negatives, FP

Table 1
***p*-values for the statistical analysis comparing RGB values on day 1 and days 2 and 3 within the same group.** The *p*-values reveal no significant differences in the RGB values between day 1 and days 2 or 3 within the same group (*p*-value >0.05).

Group	Colour	day 1 vs day2	day 1 vs day 3
Standard	Red	0.341	0.539
	Green	0.664	0.208
	Blue	0.275	0.684
Counterfeit	Red	0.459	0.445
	Green	0.849	0.415
	Blue	0.878	0.742

indicates false positives, and FN represents false negatives. The subscript i indicates the number zero or one, symbolising the absence or presence of the colouring solution, respectively. Thus, zero represents standard and one represents counterfeit, with n indicating the number of classes. Sensitivity and specificity serve as vital measures of the model's capability to accurately identify true positive and negative outcomes respectively, offering insights into the reliability and effectiveness of the classification model. We also employed the F1-score, a harmonic mean of the precision and recall, to assess the overall performance of the model. Furthermore, the AUC was calculated to evaluate the model's capacity to distinguish between positive and negative classes. Each model was trained and validated through 10 iterations, and the classification performance was assessed based on these metrics.

2.8. Visualising regions significantly affecting the model's decision

Grad-CAM is a visualisation technique that assists in identifying the critical regions of input data focused upon by a neural network during the classification process (Selvaraju et al., 2017). This method harnesses the gradient information flowing into the convolutional layer of a neural network related to a target class in order to create a heatmap. This heatmap accentuates the regions of the input data of utmost importance by the feature map's significance and representing it using different colours. Heatmap analysis provides valuable insights into the key aspects of the input data that contribute to the classification decision.

In the current study, Grad-CAM was employed to explore the influence of spectral data on the classification of standard versus counterfeit beef. This method was applied to the last convolutional layer of the AlexNet involved in spectral data processing. This generated a heatmap, highlighting the pertinent regions of the input spectra in red and the less significant features in blue.

2.9. External validation

For the purpose of external validation, we utilised a distinct set of 70 beef samples, sourced from three disparate anatomical regions: rump ($n = 40$), tenderloin ($n = 20$), and chuck ($n = 10$). The rump and tenderloin samples were procured from South Korea, while the chuck samples originated from Australia. Each sample was meticulously sectioned into dimensions of 2 cm × 2 cm × 2 cm (length × width × thickness) and hermetically sealed in polyethylene sheets characterised by low oxygen permeability. To ensure a comprehensive evaluation, the rump and tenderloin samples were subjected to two divergent storage conditions. A subset, comprising 10 samples each from the rump and tenderloin categories, was stored under conditions identical to those employed for internal validation. The remaining samples were maintained at a controlled ambient temperature of 25 °C for a duration of five days. In contrast, the chuck samples were stored at a controlled temperature of 25 °C for a period of three days. The diffuse reflectance spectra (R_{sample}) of beef samples were acquired in the same manner as explained in section 2.4, with the exception that multiple points on the beef samples were measured. This approach resulted in a total of 600 data, consisting of 300 counterfeit samples and 300 standard samples. This methodological approach was meticulously designed to account for potential variability arising from differences in anatomical regions and storage conditions.

We conducted a comprehensive assessment of traditional machine learning algorithms, such as support vector machine (SVM) and logistic regression, in addition to our DL model, utilising an external dataset (LaValley et al., 2008; Pisner and Schnyer, 2020). Initially, the SVM, logistic regression, and DL models were trained on an internal dataset. Subsequently, these pre-trained models were applied to the external dataset to evaluate their robustness. This methodology enabled us to rigorously assess the performance of each model on previously unseen data.

3. Results and discussion

3.1. Statistical comparison between the standard and counterfeit groups

To ensure that the beef samples in both the standard and counterfeit groups underwent testing under consistent conditions, an independent t-test was performed on the intensity of the RGB components within each group at two distinct time points: immediately post-arrival (day 0) and pre-colouring (day 11). Generally, meat samples are highly susceptible to storage conditions and environmental influences, and results can be unreliable if these variables are not adequately controlled. The statistical comparison between the standard and counterfeit groups revealed no significant differences in the intensity of the RGB components (p-value >0.05), as illustrated in Fig. 1. These findings demonstrate the uniformity and impartiality of the experimental conditions and environmental settings for both the standard and counterfeit groups.

3.2. Trends in the red, green, and blue components during storage

To monitor the colour change of the beef samples over the storage duration, we extracted colour information from daily images of the beef samples' surfaces. Fig. 2 presents the variations in the RGB components extracted from surface images of the beef samples in both the counterfeit and standard groups from day 1 to day 11. Between day 1 and day 11, the red component gradually declined over time in both groups, whereas the blue and green components gradually increased. The changes in the RGB components on the beef surface observed throughout the storage period were congruent with those reported in previous studies (Nguyen et al., 2016; Shin et al., 2021).

However, noteworthy differences were observed in the slope of the trend line and the R^2 value. This can be attributed to variations in the storage temperature of the beef, experimental procedure, and specific cut of beef. In a prior study, the storage temperature was set at 4.5 °C (Nguyen et al., 2019), which is 0.5 °C higher than the storage conditions utilised in the current research. Moreover, the exposure of beef samples to room temperature was minimised in this study owing to the practice of spectral measurements being performed once a day, as opposed to twice daily in the previous study (Nguyen et al., 2019). Temperature is intrinsically associated with meat spoilage, with the rate of spoilage rising exponentially as the temperature increases (Davey and Gilbert, 1976). Consequently, it is reasonable that the beef samples in this study, stored at comparatively lower temperatures and exposed less frequently to room temperature, would exhibit a more gradual trend line slope.

Additionally, the former study utilised samples from various cuts such as loin, round, chuck, and brisket (Nguyen et al., 2019), whereas this study employed samples from the rump of the cows. Given that beef samples exhibit different spoilage rates due to variances in fat and moisture content across different cuts, it is plausible that the variation in sample cuts influenced the slope of the trend line and the R^2 value (Chang et al., 2012).

3.3. Preparation and validation of the colouring solution

The formulation of the colouring solution was devised based on the observed trends in the RGB colour components, as illustrated in Fig. 2. Both the counterfeit and standard beef samples exhibited a gradual decrease in the red component over time, whereas the blue and green components experienced a steady increase. Given that the colouring solution's objective was to make the beef resemble its fresh state (day 1), we aimed to enhance the red component and suppress the green and blue components. Through a series of iterative experiments, we developed an optimal recipe comprising the Red No. 40 food colourant, sodium nitrite, and sodium ascorbate to bolster the red component, as well as squid ink, a natural colouring agent, to diminish the blue and green components.

To corroborate the effectiveness of the colouring solution employed

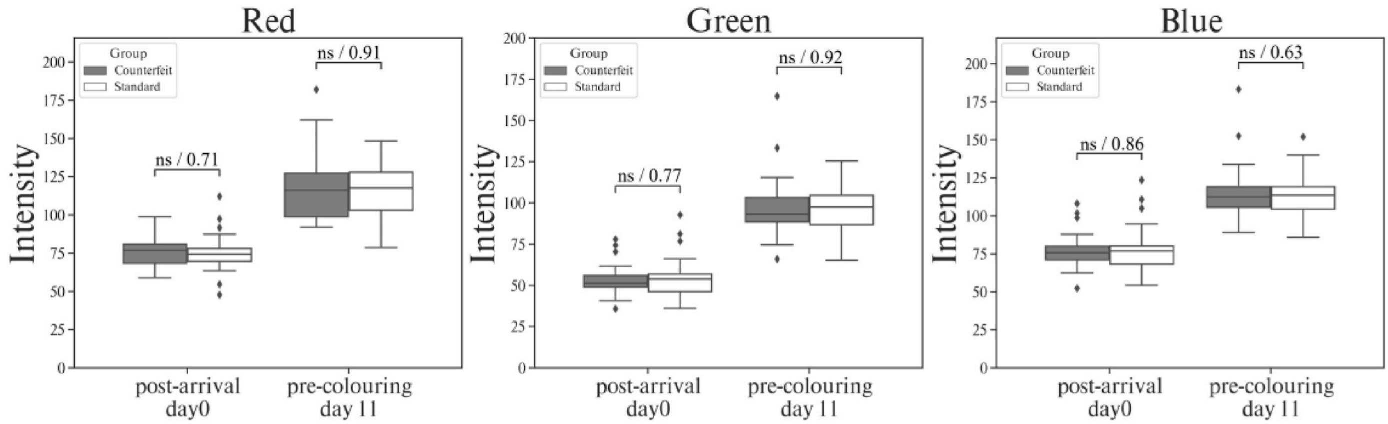

Fig. 1. Statistical comparison of the intensity of RGB components between the standard and counterfeit groups, indicated by corresponding *p*-values. The results show no significant difference (*p*-value >0.05) between the two groups.

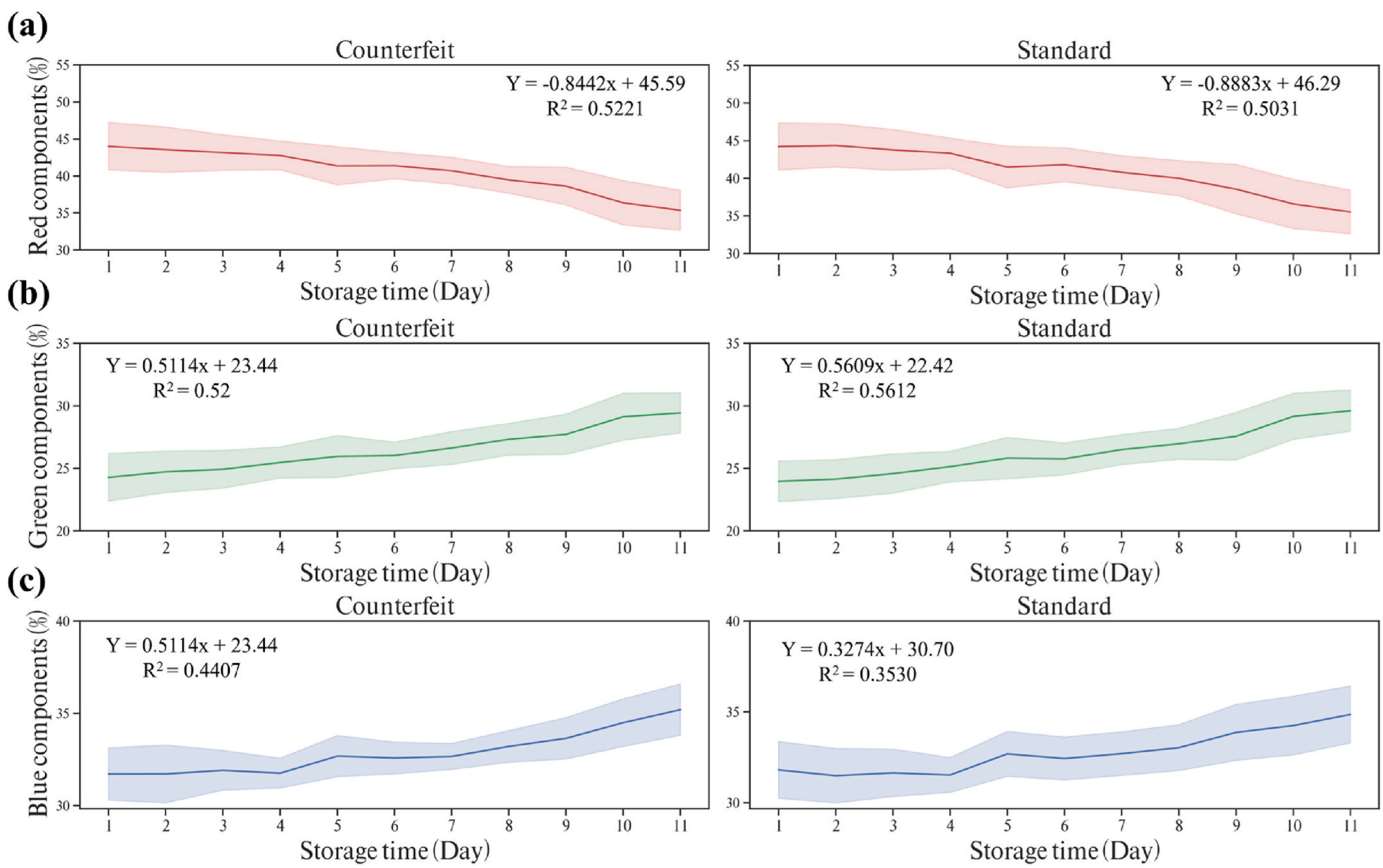

Fig. 2. Trend analysis of the RGB values of beef samples with respect to storage time: (a) red components, (b) green components, and (c) blue components. Shaded regions indicate the standard deviation. The equations within each panel represent the outcomes of linear regression analysis, with R^2 denoting the coefficient of determination. (For interpretation of the references to colour in this figure legend, the reader is referred to the Web version of this article.)

in the study, we conducted a statistical analysis focused on the intensities of the RGB components extracted from the images of the beef surfaces. The colouring solution's objective was to render the fresh (day 1) and counterfeit (day 13) beef samples visually indistinguishable. Hence, we performed a paired *t*-test with Bonferroni correction comparing the intensities of the RGB components between the beef samples from day 1 and day 13 within the counterfeit group. The *p*-values for the RGB intensities for the beef samples from day 1 and day 13 were 0.277, 0.211, and 0.101 respectively, indicating no significant differences, as demonstrated in Fig. 3 (a).

Conversely, when the same statistical analysis was applied to the day 1 and day 13 beef samples within the standard group that did not employ the colouring solution, a statistically significant difference was noted in the intensities of the RGB components, as shown in Fig. 3 (b). The *p*-values for the RGB components in the standard group were 7.80×10^{-10}, 1.71×10^{-10}, and 2.74×10^{-8} respectively.

Fig. 4 presents images and spectral information of the beef samples utilised in the experiment and offers a qualitative representation of the aforementioned statistical results. In the standard group that did not employ the colouring solution, a significant difference in colour

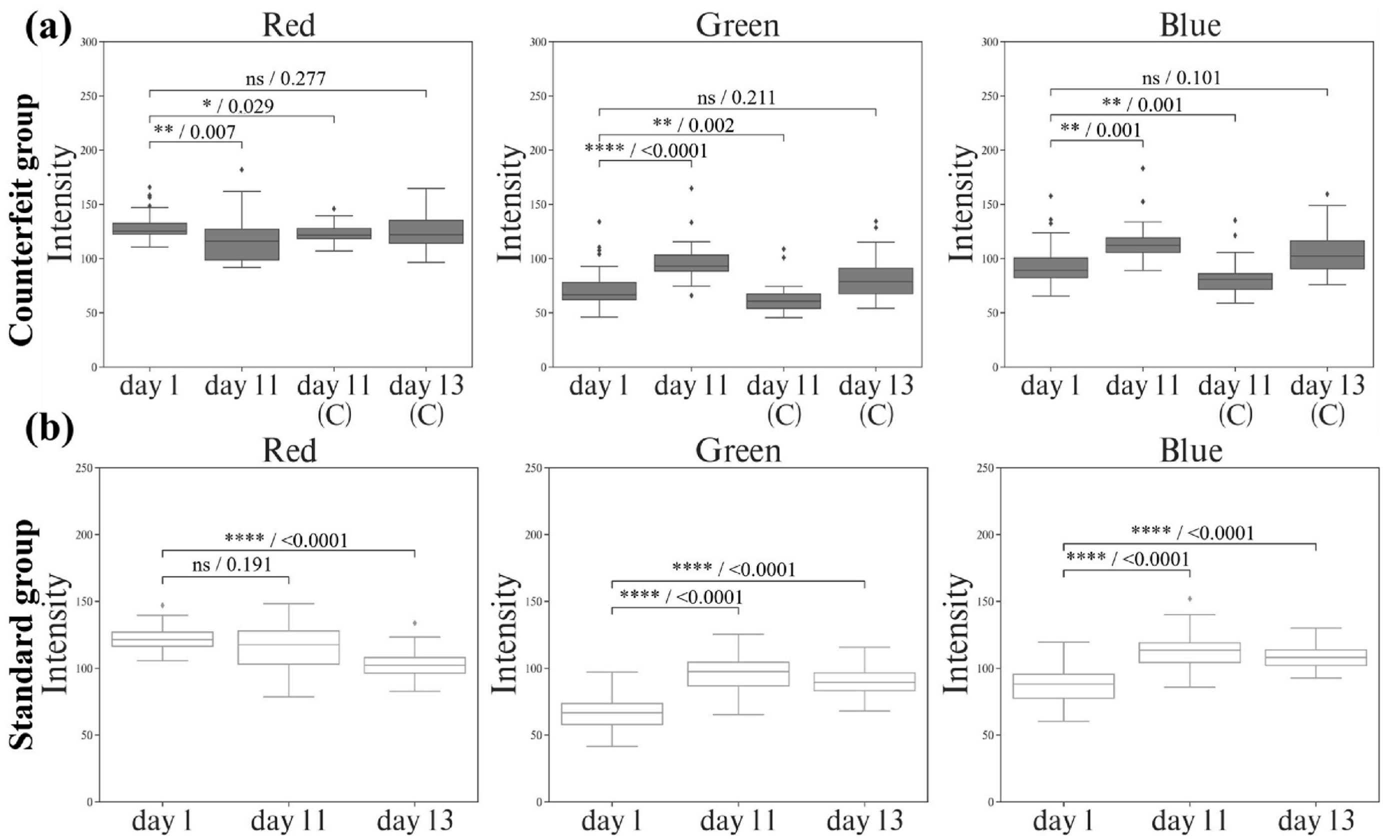

Fig. 3. Outcomes of paired t-tests conducted within each group to affirm the effectiveness of the colouring solution. (a) Beef samples treated with the colouring solution on day 11 (counterfeit group). (b) Beef samples untreated with the colouring solution (standard group). The annotations denote the results of statistical tests: ns for *p*-value >0.05, * for *p*-value ≤ 0.05, ** for *p*-value ≤ 0.01, and **** for *p*-value ≤ 0.0001. The value adjacent to the annotation indicates the respective *p*-value, and C within parentheses signifies the usage of the colouring solution.

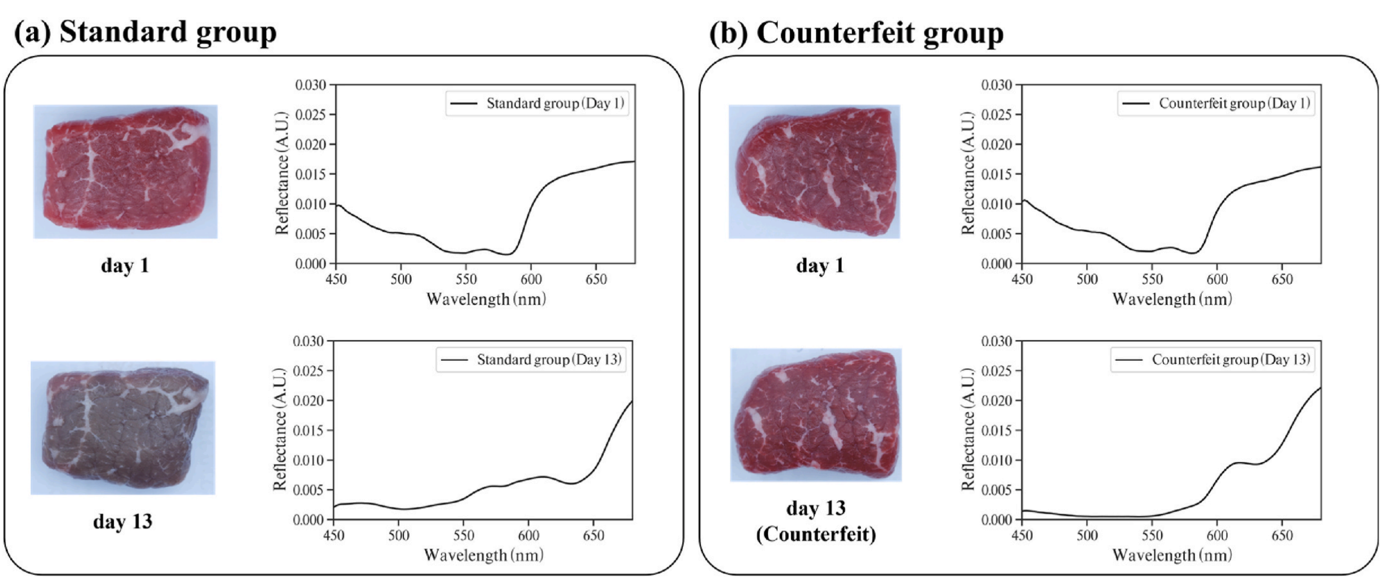

Fig. 4. Comparison of surface images and spectral information of randomly selected beef samples from the standard and counterfeit groups on day 1 and day 13. The image from the standard group on day 13 visually highlights significant deterioration in beef quality, whereas such deterioration is less discernible in the counterfeit group treated with the colouring solution.

information was evident between the two different time points, whereas the counterfeit group that employed the colouring solution exhibited no discernible difference.

These statistical results offer compelling support for the effectiveness of the colouring solution in maintaining the visual freshness of beef. By utilising the colouring solution, low-quality beef can be masqueraded as high quality, making it visually indistinguishable to consumers. Hence, these results emphasise the critical necessity for the development of technology capable of detecting counterfeit beef to thwart food fraud and safeguard consumers from potential harm.

3.4. Evaluating classification performance and constructing generalised model for data under variable conditions

In this study, we employed spectral information, which maintains a close relationship with meat quality, as input data for the development of a AlexNet-based DL model to classify standard and counterfeit beef. Furthermore, we conducted a comparative analysis, pitting our method against traditional machine learning algorithms, specifically support vector machine (SVM) and logistic regression (LaValley et al., 2008; Pisner and Schnyer, 2020). Our prior study utilised extracted myoglobin information to enhance beef freshness classification performance (Shin et al., 2021). However, in this research, we aimed to enhance the technique's practicality by solely relying on diffuse reflectance spectra, without the need for myoglobin information acquisition.

Initially, our DL model was trained using spectral data spanning from 344 nm to 1040 nm. The DL model demonstrated exceptional performance on the internal validation dataset, as depicted in Table 2. According to Table 2, the DL model achieved an impressive average accuracy of 98.84% over 10 iterations. This outstanding performance was further highlighted by a high AUC value of 0.98, as shown in Table 2, indicating the model's superior classification capability. Additionally, the model's accuracy was further confirmed with an F1-score of 0.95. These remarkable performance metrics validate the effectiveness of the proposed method in identifying counterfeit beef without the need for myoglobin information extraction, leveraging the powerful feature extraction capabilities of DL.

Despite the exceptional performance of our method, it was slightly lower than that of machine learning algorithms on the internal validation set. Nevertheless, it remains crucial to assess the algorithm's ability to capture general features for classifying counterfeit beef from a diverse range of beef cuts and under varying storage conditions in real-world scenarios. To evaluate the generalisation capability of both machine learning methods and our model, we collected an external validation set comprising various beef cuts, such as rump, tenderloin, and chuck, under various storage conditions. Interestingly, our model outperformed SVM and logistic regression on the external dataset, achieving an accuracy of 97.61%, a 0.98 AUC, a 0.98 F1-score, a 0.97 sensitivity, and a 0.99 specificity, as demonstrated in Table 2. These results underscore that our model effectively captured the general features from diverse beef samples and highlight the robustness of our proposed model for real-world applications in detecting counterfeit beef.

An intriguing avenue for future research, not directly explored in the current study, pertains to the applicability of our method in identifying meat anomalies such as PSE (Pale, Sofe, Exudative) and DFD (Dark, Firm, Dry), which are less commonly observed in beef. Numerous studies have successfully employed VIS/NIR spectroscopy to discriminate between normal, PSE, and DFD meat, reporting high classification accuracies (Jiang et al., 2017; Barbon et al., 2018; Tejerina et al., 2022). Given that our methodology also leverages spectral data in the VIS/NIR region, albeit for the detection of adulteration via colouring agents, it stands to reason that our approach may possess utility in the identification or differentiation of PSE and DFD conditions. This conjecture suggests that our method could have broader applications and highlights its relevance in the ongoing scientific discussions about meat quality assessment.

3.5. Reducing the input wavelength region: wavelength selection using Grad-CAM

To enhance the practicality and efficiency of the developed model, we employed Grad-CAM analysis to identify influential wavelength regions pertinent to the classification task. Initially, Grad-CAM was applied to a counterfeit beef classification model trained with diffuse reflectance spectra in the 344–1040 nm wavelength region to derive wavelength-dependent weights. As depicted in Fig. 5, data within the 580–600 nm wavelength region were underscored as significantly influential in classifying counterfeit beef samples. These findings align with those of a previous study that underscored the importance of the 575–600 nm region in classifying the freshness of beef (Shin et al., 2021). This observation corroborates the notion that crucial features associated with the quality of beef are concentrated in the second half of 500 nm, situated in the visible light region. To evaluate the significance of this specific wavelength region, we conducted a separate training experiment using spectral data solely within the 580–600 nm range. Notably, the model trained exclusively on this region maintained its outperforming performance, achieving an average accuracy of 97.85% (AUC: 0.97, F1: 0.93) on internal data and an accuracy of 93.94% (AUC; 0.94, F1: 0.94) on external dataset, as indicated in Table 2. This result further affirms the critical importance of the 580–600 nm wavelength region in accurately classifying standard and counterfeit beef samples, underscoring the superior capability of our model in capturing salient features from the data.

The 580–600 nm region possesses several characteristics that correlate with myoglobin information, which are not observed in other wavelength regions. Myoglobin displays different structural formations depending on its redox state (Mancini and Hunt, 2005), and these structures result in varying spectroscopic properties. Consequently, the composition of the myoglobin redox state dictates the shape of the diffuse reflectance spectra derived from meat. Generally, the myoglobin redox states present in meat are oxymyoglobin (oxy-Mb), deoxymyoglobin (deoxy-Mb), and metmyoglobin (met-Mb), which are characterised by a steep change in absorption for oxy-Mb and deoxy-Mb in the 580–600 nm region. The abruptness of the absorption indicates that

Table 2
Summary of the performance of the classification model for distinguishing between standard and counterfeit beef based on different wavelength regions on internal and external validation set, as indicated by accuracy (ACC), sensitivity, specificity, F1-score, and area under the curve (AUC). The data shown represent the mean standard deviation of the overall sample set.

Dataset	Wavelength	Algorithm	ACC (%)	AUC	F1-score	Sensitivity	Specificity
Internal	**344–1040 nm**	**SVM**	99.52 ± 0.01	0.98 ± 0.03	0.98 ± 0.04	1.00 ± 0.00	0.97 ± 0.07
		Logistic	99.05 ± 0.02	0.97 ± 0.07	0.96 ± 0.08	1.00 ± 0.00	0.93 ± 0.13
		Ours	98.84 ± 2.65	0.98 ± 0.07	0.95 ± 0.14	0.99 ± 0.02	0.96 ± 0.15
	580–600 nm	**SVM**	99.05 ± 0.02	0.99 ± 0.01	0.97 ± 0.06	0.99 ± 0.02	1.00 ± 0.00
		Logistic	99.52 ± 0.01	0.997 ± 0.01	0.99 ± 0.03	0.99 ± 0.01	1.00 ± 0.00
		Ours	97.85 ± 4.24	0.97 ± 0.08	0.93 ± 0.16	0.98 ± 0.04	0.97 ± 0.15
External	**344–1040 nm**	**SVM**	88.31	0.88	0.89	0.77	1.0
		Logistic	69.15	0.69	0.59	0.93	0.45
		Ours	**97.61**	**0.98**	**0.98**	**0.96**	**0.99**
	580–600 nm	**SVM**	86.90	0.87	0.88	0.74	1.0
		Logistic	84.79	0.85	0.87	0.70	1.0
		Ours	**93.94**	**0.94**	**0.94**	**0.88**	**0.997**

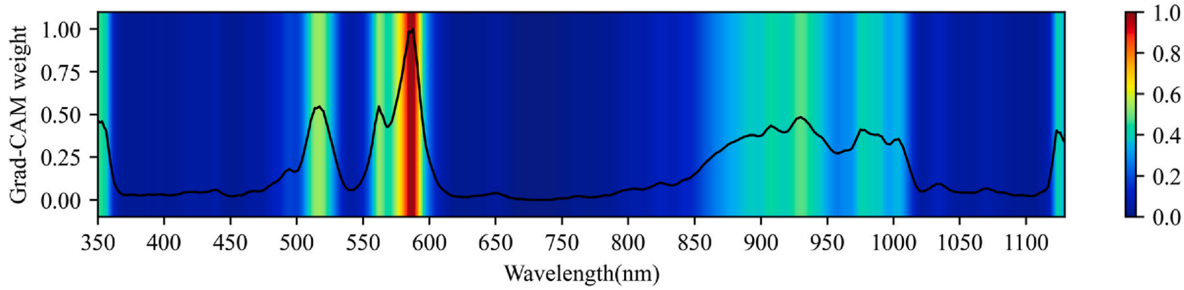

Fig. 5. Analysis of averaged Grad-CAM weights for counterfeit beef classification model. Grad-CAM result reveals a significant influence of the 580–600 nm wavelength region on the model's decision-making process. In the figure, regions highlighted in red represent wavelength areas that have a substantial impact on the model's classification, whereas those in blue indicate areas of lesser influence. (For interpretation of the references to colour in this figure legend, the reader is referred to the Web version of this article.)

the shape of their diffuse reflectance spectra can sensitively respond to minor changes in their composition. Hence, our model appears capable of detecting the differences between standard and counterfeit beef and achieving high accuracy by focusing on this particular region.

The second contributing factor lies in the existence of the isosbestic points of oxy-Mb and deoxy-Mb and oxy-Mb and met-Mb within this region. An isosbestic point denotes a juncture at which the absorption of a chromophore is equal, and a widely acknowledged method to estimate chromophore composition change involves analysing the absorption over the surrounding wavelength region based on the isosbestic point. Two available isosbestic points exist within the 580–600 nm region, likely aiding in the model's classification capacity. Contrary to previous studies that utilised an analytical photon diffusion model to directly extract myoglobin information and incorporate it as prior information (Shin et al., 2021), the present study succeeded in extracting the necessary features to discriminate counterfeit beef from diffuse reflectance spectra using only a DL model.

By restricting the spectral region, we discover several benefits, including reducing the system complexity and augmenting the practicality of our proposed method. This approach paves the way for potential real-world applications within the meat industry, where the requirement for portable equipment is often prevalent.

4. Conclusion

In this study, we have developed a AlexNet-based DL model that utilises spectral data for the identification of counterfeit beef, exhibiting significant potential for industrial application and real-world scenarios. The counterfeit beef samples, created using a colouring solution, did not demonstrate any statistically significant variation in colour information from the standard beef samples, indicating that consumers may find it challenging to visually differentiate between counterfeit and standard beef. However, our proposed method managed to distinguish the counterfeit beef from the standard beef with remarkable accuracy, suggesting that the spectral data contained crucial information for distinguishing counterfeit beef, and that our model was successful in extracting these pertinent features. Notably, our proposed method demonstrated superior performance across various conditioned beef samples, thereby affirming its robustness in comparison to traditional machine learning algorithms.

Furthermore, we deployed Grad-CAM to ascertain the wavelength regions most pertinent to the classification of counterfeit beef. The findings highlighted the 580–600 nm region as the most consequential for this classification, with our model exhibiting high performance within this narrowed wavelength region. These results underscore the practicality and efficiency of our proposed method, and we anticipate that our research can significantly contribute to safeguarding consumer health against counterfeit beef and mitigating food fraud.

CRediT authorship contribution statement

Eunjung Jo: Conceptualization, Methodology, Validation, Investigation, Data processing, Writing – original draft, Visualization. **Youngjoo Lee:** Conceptualization, Methodology, Validation, Investigation, Data processing, Writing – original draft, Visualization. **Yumi Lee:** Methodology, Investigation. **Jaewoo Baek:** Methodology, Investigation. **Jae Gwan Kim:** Conceptualization, Resources, Writing – review & editing.

Declaration of competing interest

The authors declare that they have no known competing financial interests or personal relationships that could have appeared to influence the work reported in this paper.

Data availability

Data will be made available on request.

Acknowledgements

This work was supported by the GIST Research Institute (GRI) Integrated Institute of Biomedical Research (IIRB) grant funded by the GIST in 2023. This work was also supported by the National Research Foundation of Korea (NRF) grant funded by the Korea government (MSIT) (2022K1A3A1A20014975).

References

Agelet, L.E., Hurburgh Jr., C.R., 2010. A tutorial on near infrared spectroscopy and its calibration. Crit. Rev. Anal. Chem. 40 (4), 246–260.
Aernouts, B., Polshin, E., Lammertyn, J., Saeys, W., 2011. Visible and near-infrared spectroscopic analysis of raw milk for cow health monitoring: reflectance or transmittance? J. Dairy Sci. 94, 5315–5329.
Barai, B., Nayak, R., Singhal, R., Kulkarni, P., 1992. Approaches to the detection of meat adulteration. Trends Food Sci. Technol. 3, 69–72.
Barbon, S., Costa Barbon, A.P.A.D., Mantovani, R.G., Barbin, D.F., 2018. Machine learning applied to near-infrared spectra for chicken meat classification. J.Spectros.
Barciela, P., Perez-Vazquez, A., Prieto, M., 2023. Azo dyes in the food industry: features, classification, toxicity, alternatives, and regulation. Food Chem. Toxicol., 113935
Bjelanovic, M., Egelandsdal, B., Phung, V., Langsrud, Ø., Sørheim, O., Hunt, M., Slinde, E., 2016. Effects of metabolic substrates on myoglobin redox forms in packaged ground beef. Food Packag. Shelf Life 8, 24–32.
Cavin, C., Cottenet, G., Cooper, K.M., Zbinden, P., 2018. Meat vulnerabilities to economic food adulteration require new analytical solutions. Chimia 72, 697–697.
Chakravartula, S.S.N., Moscetti, R., Bedini, G., Nardella, M., Massantini, R., 2022. Use of convolutional neural network (cnn) combined with ft-nir spectroscopy to predict food adulteration: a case study on coffee. Food Control 135, 108816.
Chang, Z., Zheng, D.M., Xia, X.F., Kong, B.H., 2012. Quality attributes of four major retails cuts from songjiang cattle. Adv. Mater. Res. 554, 1160–1164.
Clofent, D., de Homdedeu, M., Muñoz-Esquerre, M., Cruz, M.J., Muñoz, X., 2020. Sudan red dye: a new agent causing type-2 occupational asthma. Allergy Asthma Clin. Immunol. 16, 1–3.

Corlett, M.T., Pethick, D.W., Kelman, K.R., Jacob, R.H., Gardner, G.E., 2021. Consumer perceptions of meat redness were strongly influenced by storage and display times. Foods 10, 540.

Crowe, W., Elliott, C.T., Green, B.D., 2019. A review of the in vivo evidence investigating the role of nitrite exposure from processed meat consumption in the development of colorectal cancer. Nutrients 11, 2673.

Davey, C.L., Gilbert, K.V., 1976. The temperature coefficient of beef ageing. J. Sci. Food Agric. 27, 244–250.

Desmond, E., 2006. Reducing salt: a challenge for the meat industry. Meat Sci. 74, 188–196.

Drugman, T., Stylianou, Y., Kida, Y., Akamine, M., 2015. Voice activity detection: merging source and filter-based information. IEEE Signal Process. Lett. 23, 252–256.

Epley, R.J., Addis, P.B., Warthesen, J.J., 1992. Nitrite in Meat. University of Minnesota Extension Service.

Fengou, L.C., Lianou, A., Tsakanikas, P., Mohareb, F., Nychas, G.J.E., 2021. Detection of meat adulteration using spectroscopy-based sensors. Foods 10, 861.

Firmani, P., De Luca, S., Bucci, R., Marini, F., Biancolillo, A., 2019. Near infrared (nir) spectroscopy-based classification for the authentication of darjeeling black tea. Food Control 100, 292–299.

Font-i Furnols, M., Guerrero, L., 2014. Consumer preference, behavior and perception about meat and meat products: an overview. Meat Sci. 98, 361–371.

Gautam, A., Raman, B., 2021. Towards effective classification of brain hemorrhagic and ischemic stroke using cnn. Biomed. Signal Process Control 63, 102178.

Giana, H.E., Silveira, L., Zângaro, R.A., Pacheco, M.T.T., 2003. Rapid identification of bacterial species by fluorescence spectroscopy and classification through principal components analysis. J. Fluoresc. 13, 489–493.

Gowen, A.A., O'Donnell, C.P., Cullen, P.J., Downey, G., Frias, J.M., 2007. Hyperspectral imaging–an emerging process analytical tool for food quality and safety control. Trends Food Sci. Technol. 18 (12), 590–598.

Hassoun, A., Sahar, A., Lakhal, L., Aït-Kaddour, A., 2019. Fluorescence spectroscopy as a rapid and non-destructive method for monitoring quality and authenticity of fish and meat products: impact of different preservation conditions. Lwt 103, 279–292.

He, K., Zhang, X., Ren, S., Sun, J., 2016. Deep residual learning for image recognition. In: Proceedings of the IEEE Conference on Computer Vision and Pattern Recognition, pp. 770–778.

Hellberg, R.S., Everstine, K., Sklare, S.A., 2020. Food Fraud: a Global Threat with Public Health and Economic Consequences. Academic Press.

Hong, E., Lee, S.Y., Jeong, J.Y., Park, J.M., Kim, B.H., Kwon, K., Chun, H.S., 2017. Modern analytical methods for the detection of food fraud and adulteration by food category. J. Sci. Food Agric. 97, 3877–3896.

Huang, H., Liu, L., Ngadi, M.O., 2014. Recent developments in hyperspectral imaging for assessment of food quality and safety. Sensors 14 (4), 7248–7276.

Islam, M.Z., Islam, M.M., Asraf, A., 2020. A combined deep cnn-lstm network for the detection of novel coronavirus (covid-19) using x-ray images. Inform. Med. Unlocked 20, 100412.

Jia, C., Jukes, D., 2013. The national food safety control system of China–a systematic review. Food Control 32, 236–245.

Jiang, H., Yoon, S.C., Zhuang, H., Wang, W., Yang, Y., 2017. Evaluation of factors in development of Vis/NIR spectroscopy models for discriminating PSE, DFD and normal broiler breast meat. Br. Poultry Sci. 58 (6), 673–680.

Jogin, M., Madhulika, M.S., Divya, G.D., Meghana, R.K., Apoorva, S., 2018. Feature extraction using convolution neural networks (CNN) and deep learning. In: 2018 3rd IEEE International Conference on Recent Trends in Electronics, Information & Communication Technology (RTEICT). IEEE, pp. 2319–2323.

Johnson, R., 2014. Food Fraud and Economically Motivated Adulteration of Food and Food Ingredients. Congressional Research Service, 43358.

Jurgens, K.D., Papadopoulos, S., Peters, T., Gros, G., 2000. Myoglobin: just an oxygen store or also an oxygen transporter? Physiology 15, 269–274.

Kamruzzaman, M., Makino, Y., Oshita, S., 2016. Rapid and non-destructive detection of chicken adulteration in minced beef using visible near- infrared hyperspectral imaging and machine learning. J. Food Eng. 170, 8–15.

Krizhevsky, A., Sutskever, I., Hinton, G.E., 2012. Imagenet classification with deep convolutional neural networks. Adv. Neural Inf. Process. Syst. 25.

LaValley, M.P., 2008. Logistic regression. Circulation 117 (18), 2395–2399.

Li, D., Zang, M., Wang, S., Zhang, K., Zhang, Z., Li, X., Li, J., Guo, W., 2022. Food fraud of rejected imported foods in China in 2009–2019. Food Control 133, 108619.

Li, X., Zang, M., Li, D., Zhang, K., Zhang, Z., Wang, S., 2023. Meat food fraud risk in Chinese markets 2012–2021. npj Sci. Food 7, 12.

Liu, Y., Pu, H., Sun, D.W., 2021. Efficient extraction of deep image features using convolutional neural network (cnn) for applications in detecting and analysing complex food matrices. Trends Food Sci. Technol. 113, 193–204.

Mancini, R., Hunt, M., 2005. Current research in meat color. Meat Sci. 71, 100–121.

Mandair, G.S., Morris, M.D., 2015. Contributions of Raman Spectroscopy to the Understanding of Bone Strength.

Matveyeva, T.A., Sarimov, R.M., Simakin, A.V., Astashev, M.E., Burmistrov, D.E., Lednev, V.N., Sdvizhenskii, P.A., Grishin, M.Y., Pershin, S.M., Chilingaryan, N.O., et al., 2022. Using fluorescence spectroscopy to detect rot in fruit and vegetable crops. Appl. Sci. 12, 3391.

Meenu, M., Xu, B., 2019. Application of vibrational spectroscopy for classification, authentication and quality analysis of mushroom: a concise review. Food Chem. 289, 545–557.

Mishra, P., Singh, U., Pandey, C.M., Mishra, P., Pandey, G., 2019. Application of student's t-test, analysis of variance, and covariance. Ann. Card Anaesth. 22, 407.

Mitsumoto, M., Maeda, S., Mitsuhashi, T., Ozawa, S., 1991. Near-infrared spectroscopy determination of physical and chemical characteristics in beef cuts. J. Food Sci. 56, 1493–1496.

Moon, E.J., Kim, Y., Xu, Y., Na, Y., Giaccia, A.J., Lee, J.H., 2020. Evaluation of salmon, tuna, and beef freshness using a portable spectrometer. Sensors 20, 4299.

Nguyen, T., Kim, J.G., 2019. A simple but quantitative method for non-destructive monitoring of myoglobin redox forms inside the meat. J. Food Sci. Technol. 56, 5354–5361.

Nguyen, T., Kim, S., Kim, J.G., 2019. Diffuse reflectance spectroscopy to quantify the met-myoglobin proportion and meat oxygenation inside of pork and beef. Food Chem. 275, 369–376.

Nguyen, T., Phan, K.N., Lee, J.B., Kim, J.G., 2016. Met-myoglobin formation, accumulation, degradation, and myoglobin oxygenation monitoring based on multiwavelength attenuance measurement in porcine meat. J. Biomed. Opt. 21, 057002–057002.

Pan, H., Feng, J., He, G.X., Cerniglia, C.E., Chen, H., 2012. Evaluation of impact of exposure of Sudan azo dyes and their metabolites on human intestinal bacteria. Anaerobe 18, 445–453.

Petersen, M., Yu, Z., Lu, X., 2021. Application of Raman spectroscopic methods in food safety: a review. Biosensors 11, 187.

Petronijević, R.B., Velebit, B., Baltić, T., 2017. Shedding light on food fraud: spectrophotometric and spectroscopic methods as a tool against economically motivated adulteration of food. In: IOP Conference Series: Earth and Environmental Science, vol. 85. IOP Publishing, 012024, 1.

Pisner, D.A., Schnyer, D.M., 2020. Support vector machine. In: Machine Learning. Academic Press, pp. 101–121.

Qu, J.H., Liu, D., Cheng, J.H., Sun, D.W., Ma, J., Pu, H., Zeng, X.A., 2015. Crit. Rev. Food Sci. Nutr. 55, 1939–1954.

Roberts, J., Power, A., Chapman, J., Chandra, S., Cozzolino, D., 2018. A short update on the advantages, applications and limitations of hyperspectral and chemical imaging in food authentication. Appl. Sci. 8 (4), 505.

Robson, K., Dean, M., Brooks, S., Haughey, S., Elliott, C., 2020. A 20-year analysis of reported food fraud in the global beef supply chain. Food Control 116, 107310.

Santarelli, R.L., Pierre, F., Corpet, D.E., 2008. Processed meat and colorectal cancer: a review of epidemiologic and experimental evidence. Nutr. Cancer 60, 131–144.

Selvaraju, R.R., Cogswell, M., Das, A., Vedantam, R., Parikh, D., Batra, D., 2017. Grad-cam: visual explanations from deep networks via gradient-based localization. In: Proceedings of the IEEE International Conference on Computer Vision, pp. 618–626.

Shakil, M.H., Trisha, A.T., Rahman, M., Talukdar, S., Kobun, R., Huda, N., Zzaman, W., 2022. Nitrites in cured meats, health risk issues, alternatives to nitrites: a review. Foods 11, 3355.

Shin, S., Lee, Y., Kim, S., Choi, S., Kim, J.G., Lee, K., 2021. Rapid and non-destructive spectroscopic method for classifying beef freshness using a deep spectral network fused with myoglobin information. Food Chem. 352, 129329.

Spink, J., Moyer, D.C., 2013. Understanding and combating food fraud. Food Technol. 67 (1), 30–35.

Spink, J., Ortega, D.L., Chen, C., Wu, F., 2017. Food fraud prevention shifts the food risk focus to vulnerability. Trends Food Sci. Technol. 62, 215–220.

Tejerina, D., Oliván, M., García-Torres, S., Franco, D., Sierra, V., 2022. Use of near-infrared spectroscopy to discriminate DFD beef and predict meat quality traits in autochthonous breeds. Foods 11 (20), 3274.

Walsh, K.B., Blasco, J., Zude-Sasse, M., Sun, X., 2020. Visible-nir 'point'spectroscopy in postharvest fruit and vegetable assessment: the science behind three decades of commercial use. Postharvest Biol. Technol. 168, 111246.

Wang, W., Paliwal, J., 2007. Near-infrared spectroscopy and imaging in food quality and safety. Sens.Instrument. Food Qual.Saf. 1, 193–207.

Xu, G., Ren, T., Chen, Y., Che, W., 2020. A one-dimensional cnn-lstm model for epileptic seizure recognition using eeg signal analysis. Front. Neurosci. 14, 578126.

Zheng, X., Li, Y., Wei, W., Peng, Y., 2019. Detection of adulteration with duck meat in minced lamb meat by using visible near-infrared hyper- spectral imaging. Meat Sci. 149, 55–62.